The deformation units in metallic glasses revealed by stress-induced localized glass transition

L. S. Huo, J. Ma, H. B. Ke, H. Y. Bai, D. Q. Zhao et al.

Citation: J. Appl. Phys. **111**, 113522 (2012); doi: 10.1063/1.4728207
View online: http://dx.doi.org/10.1063/1.4728207
View Table of Contents: http://jap.aip.org/resource/1/JAPIAU/v111/i11
Published by the American Institute of Physics.

The deformation units in metallic glasses revealed by stress-induced localized glass transition

L. S. Huo, J. Ma, H. B. Ke, H. Y. Bai, D. Q. Zhao, and W. H. Wang[a)]
Institute of Physics, Chinese Academy of Sciences, Beijing 100190, People's Republic of China

(Received 25 February 2012; accepted 9 May 2012; published online 8 June 2012)

We report that even in quasi-static cyclic compressions in the apparent elastic regimes of the bulk metallic glasses, the precisely measured stress-strain curve presents a mechanical hysteresis loop, which is commonly perceived to occur only in high-frequency dynamic tests. A phenomenological viscoelastic model is established to explain the hysteresis loop and demonstrate the evolutions of the viscous zones in metallic glasses during the cyclic compression. The declining of the viscosity of the viscous zones to at least 1×10^{12} Pa s when stress applied indicates that stress-induced localized glass to supercooled liquid transition occurs. We show that the deformation units of metallic glasses are evolved from the intrinsic heterogeneous defects in metallic glasses under stress and the evolution is a manifestation of the stress-induced localized glass transition. Our study might provide a new insight into the atomic-scale mechanisms of plastic deformation of metallic glasses. © *2012 American Institute of Physics*. [http://dx.doi.org/10.1063/1.4728207]

I. INTRODUCTION

Metallic glasses (MGs) have stimulated extensive research interest in both fundamental science and engineering due to their unique properties and promising applications.[1–4] Remarkable progress has been achieved in the aspects of glass-forming ability, alloy performances, and atomic structure.[1–10] However, there still remain a good number of fundamental issues that are far from being fully understood. The atomic-scale mechanism of plastic deformation of MGs is the most difficult and challenging one, for that the atomic motions similar to the dislocation gliding in crystalline materials cannot be produced in MGs under stress due to their amorphous nature.[3] The deformation unit of MGs is generally perceived to be a local rearrangement of atoms that accommodate shear strain.[3,11] One popular viewpoint is the local event of cooperative shearing of atomic clusters termed "shear transformation zone" (STZ),[12] and another is the shear dilatation or free volume model.[13] Great effort has been dedicated to the identification and characterization of the deformation units of MGs. Based on the Johnson-Sawmer cooperative shearing model, a rate-jump nanoindentation technique was applied to identify the size of STZs of MGs.[11] The study of the viscoelastic behaviors of the MG micropillars using a high-frequency dynamic nanoindentation test revealed the existence of the nano-scale viscous zone enveloped by the elastic matrix.[9] Very recently, researchers using different techniques concluded that MGs are elastic heterogeneous in nano-scales,[14–16] providing strong implications about the relationship between the plastic deformation units and the heterogeneous "defects" in MGs. However, there still remain controversies about the existence and features of the flow units in MGs, and there exist significant differences between the characteristics of the deformation units probed by dynamic micropillar tests[9] and the heterogeneous defects characterized by other techniques.[15,16] There are some constraints in the dynamic micropillar tests: (1) The size of the micro- or submicro-scale samples might be comparable with that of the flow units, hence introducing a totally different deformation mode compared with the macroscopic samples[17–19]; and (2) in high-frequency dynamic tests, the responding speed and time resolution of the equipment is a latent source of the data errors.

In present work, we investigate the discovered mechanical hysteresis loops presented in quasi-static cyclic compressions (strain rates ranging from 10^{-5}/s to 10^{-3}/s) in the apparent elastic regimes of the bulk MGs, which can avoid the problems in high-frequency dynamic micropillar tests. We propose a phenomenological viscoelastic model to explain the experimental observations. We show that the emergence and variations of the hysteresis loops are more accurately related to the evolution of the deformation units in MGs. Our results clearly show the existence of the flow units and the evolution of the nanoscale deformation units in MGs under stress is a manifestation of stress-induced localized glass transition.

II. EXPERIMENTS

Bulk MGs with nominal compositions of $Zr_{52.5}Ti_5Cu_{17.9}Ni_{14.6}Al_{10}$ (Vit105) and $Mg_{61}Cu_{28}Gd_{11}$ (cylindrical rods with 5 mm in diameter) were used in the quasi-static cyclic compression tests. The Vit105 rods were prepared by arc melting and copper mold suck-casting method, and the Mg-based rods were fabricated by induction melting and copper mold injection casting. The fully glassy structures of the as-cast samples were verified by the differential scanning calorimetry (DSC; Perkin-Elmer DSC7, USA) and x-ray diffraction (Ultima IV, Cu K_α, Japan) (not shown). Crystalline alloys used for references were the stainless steel (AISI321), pure Ti, Al alloy (2024 AA), and ZrTiAlV alloy. Glassy and crystalline alloy rods with 5 mm in diameter were all cut into short compression samples ~13 mm in length. The

a)Author to whom correspondence should be addressed. Electronic mail: whw@iphy.ac.cn.

quasi-static cyclic compressions in the apparent elastic regimes of the glassy and crystalline alloys were all carried out in an Instron electromechanical testing system 3384 (Norwood, MA) at the strain rates ranging from 10^{-5} to 10^{-3}/s at room temperature. The strains of all the alloys were precisely measured directly on the specimens by the extensometer. For each alloy, at least 3 cycles of loading-unloading processes were conducted at each strain rate to make sure the reproducibility of the data, and the strain rates for a pair of loading and unloading were equal.

III. RESULTS AND DISCUSSIONS

As shown in Fig. 1, bulk MGs and crystalline alloys present different stress-strain responses in quasi-static cyclic compressions in their elastic regimes. All these stress-strain curves were obtained at a testing strain rate of $\sim 10^{-5}$/s, except the second one of ZrTi alloy ($\sim 1 \times 10^{-3}$/s) in Fig. 1(a). The inset in Fig. 1(a) shows the magnified curves in the black rectangle, which clearly presents the different stress-strain responses for MgCuGd glass and crystalline Ti; the inset in Fig. 1(b) gives the reproducibility of the data in three cycles of compressions of Vit105. We define a cyclic compression intensity $I_{CC} = \sigma_{max}/\sigma_y$ (σ_{max}, the maximum stress reached in each compression cycle, and σ_y, the yielding strength of the alloy) to normalize the compressions in different systems. The comparison of the maximum hysteresis of the unloading stress-strain curves in strain (H_{max}) for MGs and crystalline alloys at different I_{CC} is shown in Table I. From Fig. 1 and Table I, one can see that even in quasi-static cyclic compressions in the apparent elastic regimes of MGs, the stress-strain curve presents an obvious mechanical hysteresis loop, which is much smaller or cannot be observed in equivalent cyclic compressions of crystalline alloys. This indicates that the deformation in the elastic regimes of the MGs is viscoelastic, which is consistent with previous results.[9,14,20]

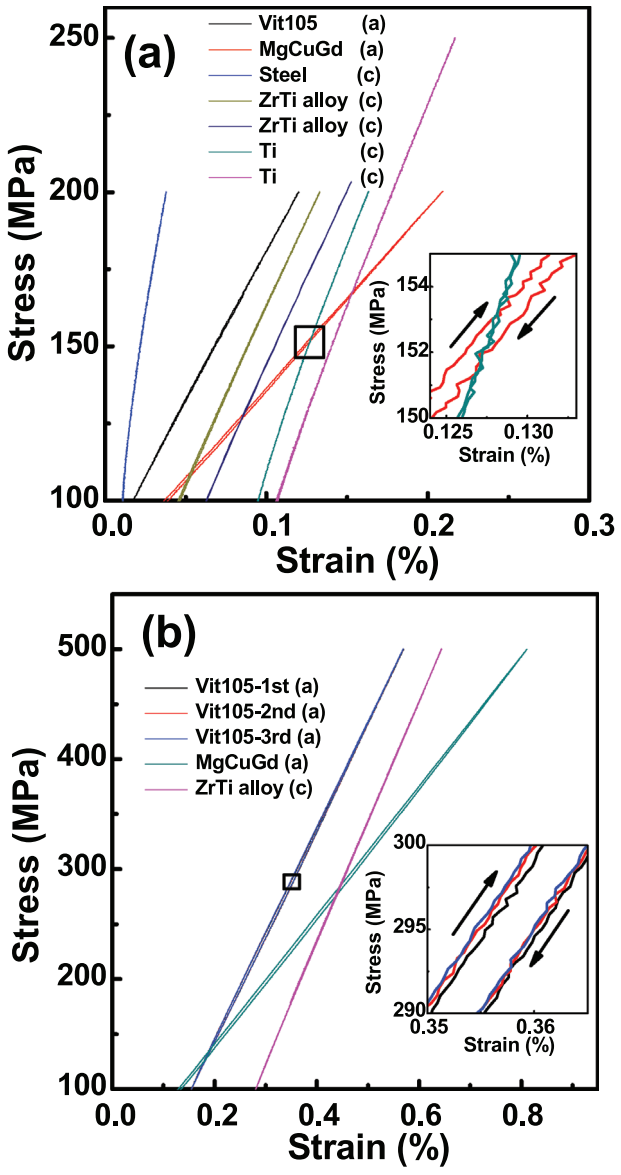

FIG. 1. (a) Different stress-strain responses of bulk MGs and crystalline alloys (represented by "*a*" and "*c*" in the brackets, respectively) in quasi-static cyclic compressions in their elastic regimes. (b) the reproducibility of the data in three cycles of compressions of Vit105. The insets show the magnified curves in the black rectangles. The loading and unloading curves are symbolized by the upward and downward arrows, respectively.

Figure 2 presents the hysteresis effect dependence on the strain rates for MGs. As presented in Figs. 2(a) and 2(b), the hysteresis loops of both Vit105 and MgCuGd in quasi-static compressions do not expand but show a certain degree of shrinkage with the strain rate increasing. The dependence of the hysteresis effect of MGs on strain rates in this work is unique compared with that obtained in high-frequency dynamic micropillar tests,[9] in which the hysteresis loop of the micropillar expands remarkably with the increase of the stress rate.

It is proposed that the macroscopic viscoelastic behavior is due to the existence of microscopic viscous zones inside the materials.[9,14,21] On the basis of the previous knowledge about the deformation unit,[3,9,12] we speculate that the viscous zones formed under stress (σ) in MGs are like the red zones illustrated in Fig. 3(a), with the blue surroundings to be the elastic matrix. Then, the MGs can be regarded to consist of the viscous liquid-like cores enveloped by the elastic

TABLE I. Comparison of H_{max} for bulk MGs and crystalline alloys at different I_{CC} ($I_{CC} = \sigma_{max}/\sigma_y$ is a cyclic compression intensity).

Material	I_{CC}	Cycles (MPa)	H_{max} (%)
Vit105 (a)	0.12	100–200	0.00125
	0.29	100–500	0.00558
	0.59	100–1000	0.00909
MgCuGd (a)	0.25	0–200	0.00234
	0.50	0–400	0.00545
	0.63	0–500	0.00758
Stainless steel (c)	0.33	0–200	~0
Ti (c)	0.54	0–200	~0
	0.68	0–250	~0
ZrTi alloy (c)	0.17	0–200	0.000698
	0.17	0–200[a]	0.000443
	0.43	0–500	0.002146

[a]This compression was conducted at the strain rate of $\sim 1 \times 10^{-3}$/s.

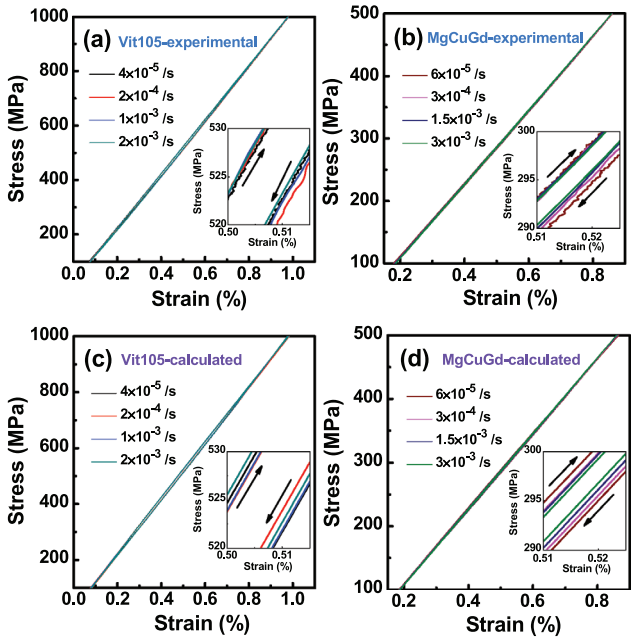

FIG. 2. The experimental cyclic compression stress-strain curves in comparison with those calculated from the fitted parameters at strain rates ranging from 10^{-5}/s to 10^{-3}/s: (a) experimental curves of Vit105 at $I_{CC} = 0.59$ ($I_{CC} = \sigma_{max}/\sigma_y$ is a cyclic compression intensity; σ_{max}, the maximum stress reached in each compression cycle; and σ_y, the yielding strength of the alloy), (b) experimental curves of MgCuGd at $I_{CC} = 0.63$, (c) calculated curves of Vit105 at $I_{CC} = 0.59$, and (d) calculated curves of MgCuGd at $I_{CC} = 0.63$. The inset in each graph shows the magnified curves and the dependence of the hysteresis on strain rate. The loading and unloading curves are symbolized by the upward and downward arrows, respectively.

solid-like shells (units like indicated in the white rectangle). The physical description of such a single deformation unit is given in Fig. 3(b). The viscous core can be considered to be a dashpot and the surroundings to be the elastic springs. Actually, the elastic components in parallel and in series with the viscous core (from the perspective of the applied stress) behave differently upon the applied stress. A viscoelastic model for the deformation unit is derived through further simplification, as shown in Fig. 3(c). E_{1eff} and E_{2eff} are the effective moduli of the elastic components in parallel and in series with the viscous core, respectively, and η_{eff} denotes the effective viscosity of the viscous core. The governing equation for such a model is expressed as[22]

$$\sigma = E_{1eff}\varepsilon - \frac{\eta_{eff}}{E_{2eff}}\frac{d\sigma}{dt} + \eta_{eff}\frac{E_{1eff}+E_{2eff}}{E_{2eff}}\frac{d\varepsilon}{dt}, \qquad (1)$$

where σ, ε, and t represent the applied stress, strain, and time, respectively.

The E_{1eff}, E_{2eff}, and η_{eff} are all the effective parameters of each part to the whole unit. We then obtain $E_{1eff} = (1-\chi)E_0$, $E_{2eff} = \chi E_0$, and $\eta_{eff} = \chi\cdot\eta$, where E_0 is the elastic modulus of the solid-like shell in the MGs, η is the averaged viscosity of the liquid-like cores, and χ is the areal fraction of the liquid-like cores in MGs. Substitution of E_{1eff}, E_{2eff}, and η_{eff} into Eq. (1) yields

$$\sigma(t) = (1-\chi)E_0\varepsilon(t) - \frac{\eta}{E_0}\frac{d\sigma(t)}{dt} + \eta\frac{d\varepsilon(t)}{dt}. \qquad (2)$$

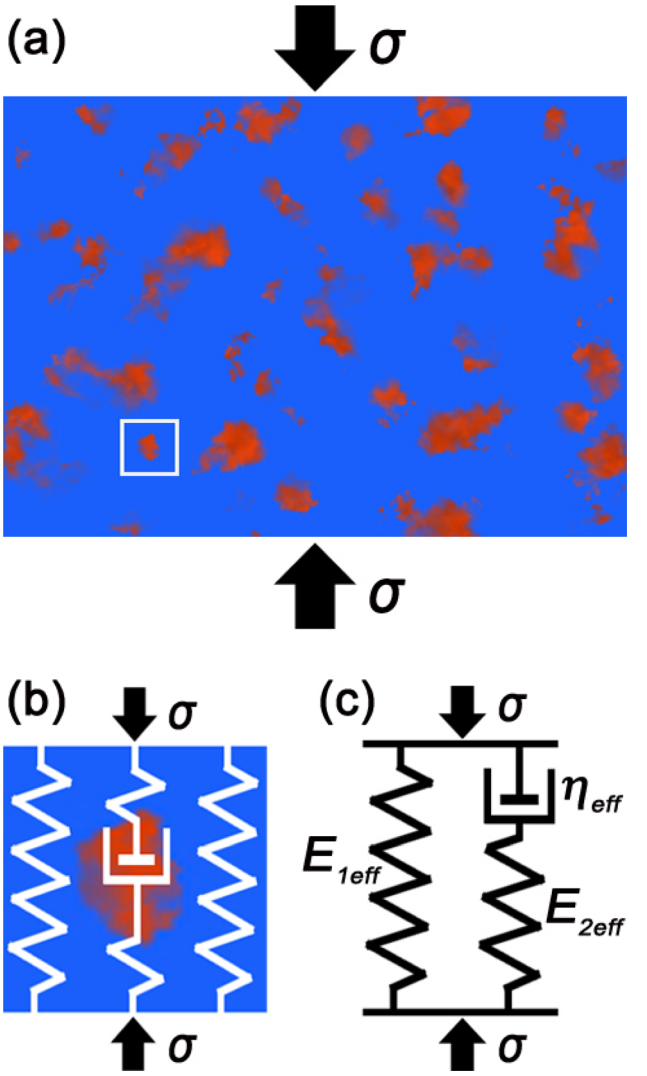

FIG. 3. Schematic diagram of deriving the viscoelastic model from the deformation unit hypothesis of MGs. (a) Distributions of the hypothetic viscous zones in MGs under stress. (b) Physical model depiction for a single deformation unit of MGs. (c) The derived viscoelastic model.

As our cyclic compression tests were all displacement-controlled, the strain-time relationship for each loading/unloading process actually slightly deviates from the ideal linearity, and is expressed perfectly with the following equation:

$$\varepsilon = A\cdot\exp\left(-\frac{t-t_0}{\tau}\right) + B, \qquad (3)$$

where A, B, τ, and t_0 are all known constants for each loading/unloading process (not shown). With Eqs. (2) and (3), we obtain the stress-strain relationship for a single loading or unloading process:

$$\sigma = E_0\cdot\frac{(1-\chi)E_0\cdot\tau-\eta}{E_0\cdot\tau-\eta}\cdot\varepsilon + \frac{\chi\eta BE_0}{E_0\cdot\tau-\eta} + C \cdot exp\left(-\frac{E_0\cdot t_0}{\eta}\right)\cdot\left(\frac{\varepsilon-B}{A}\right)^{\frac{E_0\cdot\tau}{\eta}}, \qquad (4)$$

where C is a constant generated in solving the differential equation (2). If we investigate the averaged values of E_0, η,

and χ during a cycle, these parameters can be regarded as 3 constant unknowns, and Eq. (4) actually is a simple expression as following:

$$\sigma = a1 \cdot \varepsilon + a2 + a3 \cdot \left(\frac{\varepsilon - B}{A}\right)^{a4}, \quad (5)$$

with 4 constants ($a1$, $a2$, $a3$, and $a4$).

Through the iterative fitting of the experimental stress-strain curves of Vit105 at $I_{CC} = 0.59$ and MgCuGd at $I_{CC} = 0.63$, Eq. (4) can express the experimental curves perfectly. Unlike the case that the fitted parameters are independent of the stress rate in the high-frequency dynamic tests,[9] here, the η and χ are strain rate dependent, and E_0 is strain rate independent. At higher strain rates ($\sim 10^{-3}$/s), the fitted value of η is in the order of 10^{12} Pa s, whereas at lower strain rates ranging from 10^{-5} to 10^{-4}/s, the extracted η is $\sim 10^{13}$ Pa s. This result implies that the viscosity of the viscous cores under stress reaches the value around the glass transition temperature (T_g) of MGs[23–25] and varies with the extending of the unloading time (t_u). The intrinsic differences between the defects and the surroundings are far from the viscosity variations between the viscous cores and the elastic shells under stress.[15,16]

To quantitatively clarify the variation of the viscous zones in MGs, we assumed that the viscosity of the viscous cores during a cycle of compression could be averaged to a constant value, e.g., 1×10^{12} Pa s at higher strain rates and 3×10^{13} Pa s at lower strain rates, as listed in Table II, and focused on the change of the volume fraction (v) of the cores with the fixed viscosity. By fitting the experimental stress-strain curves of Vit105 at $I_{CC} = 0.59$ and MgCuGd at $I_{CC} = 0.63$ with Eq. (4), the E_0 and χ in different compressions were extracted. And then, the v in each cyclic compression was computed from the fitted χ. The E_0, χ, and v obtained in compressions with the same strain rate were averaged and tabulated in Table II. The calculated stress-strain curves for Vit105 and MgCuGd at different strain rates using the fitted E_0, χ, and the corresponding viscosity are shown in Figs. 2(c) and 2(d). From the comparison of the experimental and calculated curves given in Figs. 2(a)–2(d), one can see that the present model and the fitted parameters have perfectly explained the mechanical hysteresis and captured the structural features of the deformation units of MGs.

TABLE II. The fitted E_0, χ, and v for the Vit105 and MgCuGd MGs at different strain rates with $I_{CC} = 0.59$ and 0.63, respectively.

			Unloading			Loading		
Materials	Strain rate (s^{-1})	η (Pa s)	E_0 (GPa)	χ (%)	v (%)	E_0 (GPa)	χ (%)	v (%)
Vit105	4×10^{-5}	3×10^{13}	92.4	9.77	2.30	104.6	11.2	2.82
	2×10^{-4}	3×10^{13}	98.3	16.8	5.18	101.5	18.2	5.84
	1×10^{-3}	1×10^{12}	93.1	6.45	1.23	103.4	6.75	1.32
	2×10^{-3}	1×10^{12}	94.5	19.2	6.31	105.6	20.8	7.14
MgCuGd	6×10^{-5}	3×10^{13}	56.2	31.1	13.1	61.7	34.1	15.0
	3×10^{-4}	3×10^{13}	58.7	32.4	13.9	59.6	29.6	12.1
	1.5×10^{-3}	1×10^{12}	57.8	15.9	4.76	60.4	14.3	4.05
	3×10^{-3}	1×10^{12}	58.7	17.2	5.38	60.2	15.2	4.46

Figure 4(a) presents the averaged values of the volume fractions of the viscous zones with the viscosity of 1×10^{12} Pa s and 3×10^{13} Pa s in Vit105 and MgCuGd, respectively, as a function of strain rate (unloading time t_u). The corresponding fitted E_0 at different strain rates is plotted in Fig. 4(b), and the Young's modulus of each alloy measured by the ultrasonic method at room temperature is given for comparison. As shown in Fig. 4, the viscous zones with the viscosity of 1×10^{12} Pa s cannot be detected at lower strain rates ($<1 \times 10^{-3}$/s for Vit105 and $\leq 10^{-4}$/s for MgCuGd), and only zones with the viscosity of 3×10^{13} Pa s can be probed. Despite the large difference of $\sim$10% between the data fitted from loading and unloading occasionally, two

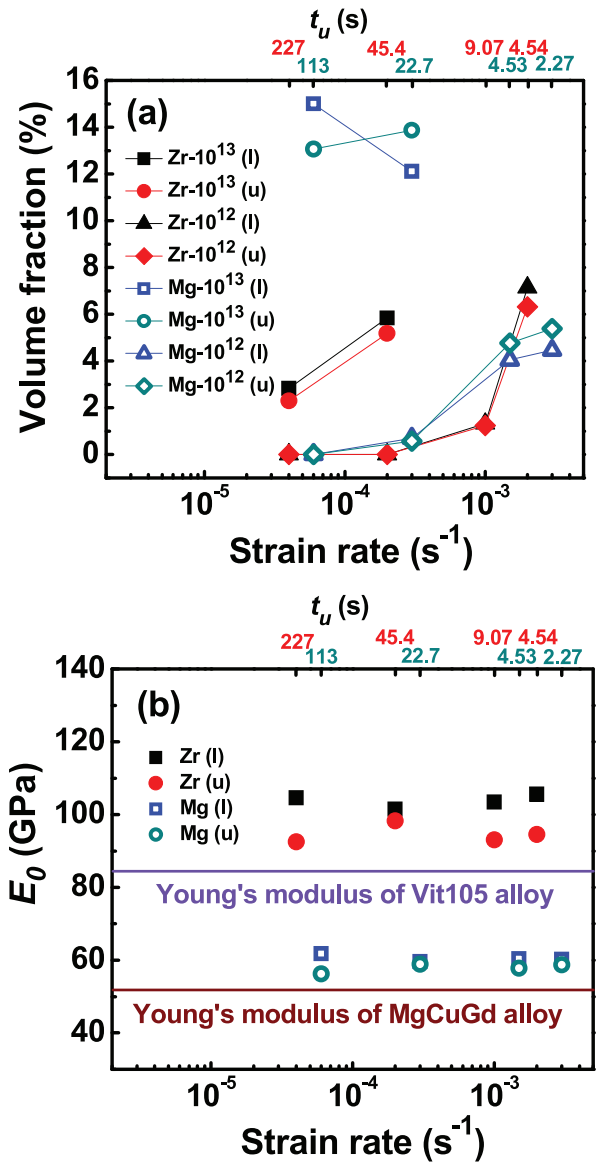

FIG. 4. The fitted parameters of the deformation units in Vit105 and MgCuGd MGs as a function of strain rate (unloading time t_u): (a) the dependence of the volume fractions of the detected viscous zones (with viscosity values 1×10^{12} Pa s and 3×10^{13} Pa s, respectively) in MGs on strain rate, (b) the fitted E_0 as a function of strain rate. The t_u in red are the unloading times for Vit105 and the green are those for MgCuGd. The "l" and "u" in the brackets represent the loading and unloading, respectively.

apparent tendencies with the strain rate varying are presented: (1) The elastic modulus of the solid-like shells (E_0) is strain rate independent as stated above, and higher than the Young's modulus of the overall sample that contains the contribution of the viscous cores, which is consistent with the previous results[9]; and (2) the detected volume fraction of the viscous cores with a certain viscosity declines and the detectable viscosity increases with the extending of the unloading time. The second tendency indicates that the viscosity of the viscous cores in MGs gradually increases and the volume of the viscoelastic zones declines when the stress is unloaded, which have been experimentally observed.[26] The evolutions are speculated to be opposite if the stress is loaded.

Recent studies have experimentally confirmed that MGs are intrinsically heterogeneous in nano-scales with fluctuations in the local modulus, viscosity, packing density, and potential energy state, which are much more significant than that in their crystalline counterparts.[14–16] The heterogeneity of MGs is schematically illustrated in Fig. 5(a). The violet and pink atom areas represent the heterogeneous defects in MGs with higher potential energies and looser packing densities compared with the relatively homogenous matrix denoted by the blue atoms. It is popularly accepted that these defect zones are the preferred sites for the activations of the atomic cluster motions caused by the applied stress or high temperatures.[15,27] On the basis of previous and present results, we propose that the viscous cores of the deformation units in MGs under stress originate from these local defects, as illustrated in Fig. 5. When the stress is applied, the atom rearrangements initiate preferably in these active zones and cause the local potential energy elevated further and the viscosity of these zones declining, which is schematically illustrated by the emerging of the higher-energy red atoms and the spread of pink atom areas. Meanwhile, the volume of the viscous zones is enlarged as the applied stress increases. The viscosity of the defect regions under stress can drop to at least 10^{12} Pa s, corresponding to the local temperature raised to T_g or even higher.[23–25] Hence the stress-induced localized glass to supercooled liquid state transition is actually a result and also a manifestation of the evolution process from the intrinsic heterogeneity of MGs to the deformation unit under stress. The variations are reversed in unloading, exhibiting the relaxation of the high energy state. Then, the localized glass transition on loading and relaxation when unloading capture the characteristics and evolution of the plastic units.[3] For the tests fast enough, such as the high-frequency dynamic tests, in which the cycling time is shorter than the relaxation time of the deformation units, the probed viscosity of the viscous zones is thus strain rate independent and lower than 1×10^{12} Pa s.[9]

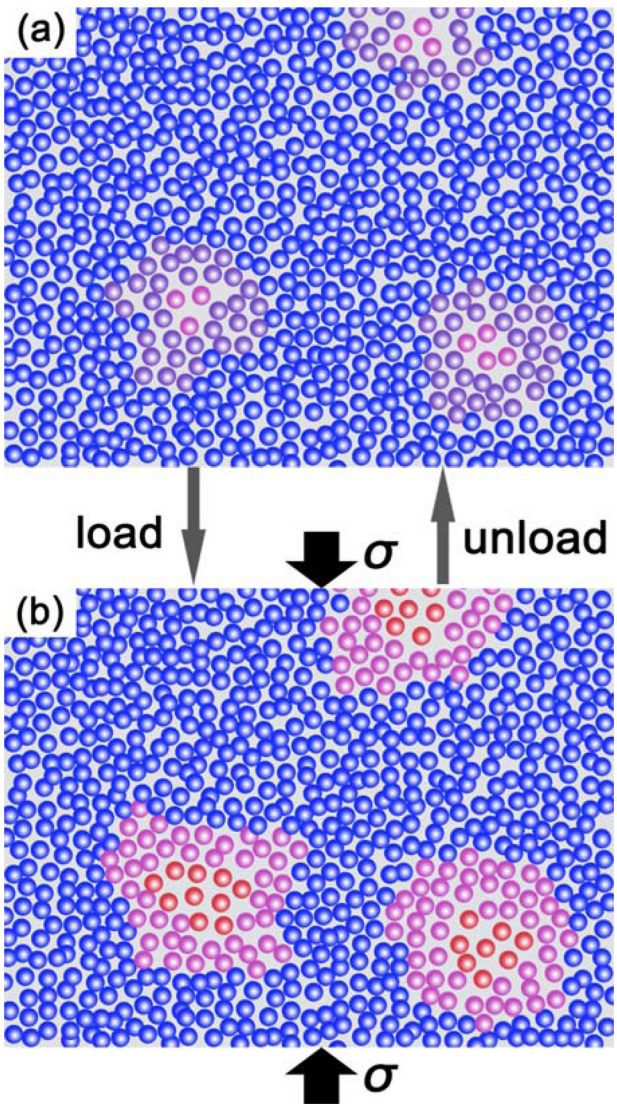

FIG. 5. Schematic illustration of the evolution from the localized heterogeneous defects to the viscous cores of the deformation units in MGs under stress. (a) The localized heterogeneous defects in MGs. (b) The viscous zones formed in MGs when stress applied. The energy state subsequence for the atoms (from low to high) is blue, violet, pink, and red.

As the volume of the viscous zones expands with the increase of stress, it is expected that when the stress increases to a certain value, the separate viscous zones will merge together into a shear band in MGs. This is supported by the experimental observations and simulations, which show that the temperature in shear bands of MGs is equal to or even higher than T_g.[28–33] On the other hand, as shown in Fig. 4(a), the descending of the volume fraction of the viscous zones for Vit105 is faster than that for MgCuGd with the extending of t_u. This is due to the faster relaxation of the viscous zones in Vit105, which indicates that the evolution of the deformation units in Vit105 is much faster and easier than that in MgCuGd. The result is consistent with the experimental observations of the generation of more shear bands and thus better plastic deformability in Vit105 compared with that in MgCuGd.[3]

IV. CONCLUSIONS

In summary, we find the mechanical hysteresis loop in the quasi-static cyclic compressions of bulk MGs by precisely recording the strain and establish a viscoelastic model to explain the loop. The variations of the viscosity of the viscous zones with the extending of unloading time indicate that localized glass to supercooled liquid state transition occurs when stress applied. We demonstrate that the

deformation units of MGs are evolved from the intrinsic heterogeneous defects.

ACKNOWLEDGMENTS

This work was supported by MOST 973 of China (No. 2010CB731603) and the NSF of China (50921091). The useful discussions and experimental help from D. W. Ding, J. G. Wang, and Z. Wang are appreciated.

[1]W. L. Johnson, Mater. Res. Bull. **24**, 42 (1999).
[2]T. Egami, Prog. Mater. Sci. **56**, 637 (2011).
[3]C. A. Schuh, T. C. Hufnagel, and U. Ramamurty, Acta Mater. **55**, 4067 (2007).
[4]W. H. Wang, Adv. Mater. **21**, 4524 (2009).
[5]D. Klaumunzer, A. Lazarev, R. Maaß, F. H. Dalla Torre, A. Vinogradov, and J. F. Loffler, Phys. Rev. Lett. **107**, 185502 (2011).
[6]D. B. Miracle, Nature Mater. **3**, 697 (2004).
[7]Y. Q. Cheng, A. J. Cao, H. W. Sheng, and E. Ma, Acta Mater. **56**, 5263 (2008).
[8]M. L. Falk and J. S. Langer, Phys. Rev. E **57**, 7192 (1998).
[9]J. C. Ye, J. Lu, C. T. Liu, Q. Wang, and Y. Yang, Nature Mater. **9**, 619 (2010).
[10]H. L. Peng, M. Z. Li, and W. H. Wang, Phys. Rev. Lett. **106**, 135503 (2011).
[11]D. Pan, A. Inoue, T. Sakurai, and M. W. Chen, Proc. Natl. Acad. Sci. U.S.A. **105**, 14769 (2008).
[12]A. S. Argon, Acta Metall. **27**, 47 (1979).
[13]F. Spaepen, Acta Metall. **25**, 407 (1977).
[14]W. Dmowski, T. Iwashita, C.-P. Chuang, J. Almer, and T. Egami, Phys. Rev. Lett. **105**, 205502 (2010).
[15]Y. H. Liu, D. Wang, K. Nakajima, W. Zhang, A. Hirata, T. Nishi, A. Inoue, and M. W. Chen, Phys. Rev. Lett. **106**, 125504 (2011).
[16]H. Wagner, D. Bedorf, S. Küchemann, M. Schwabe, B. Zhang, W. Arnold, and K. Samwer, Nature Mater. **10**, 439 (2011).
[17]H. Guo, P. F. Yan, Y. B. Wang, J. Tan, Z. F. Zhang, M. L. Sui, and E. Ma, Nature Mater. **6**, 735 (2007).
[18]A. Bharathula, S. W. Lee, W. J. Wright, and K. M. Flores, Acta Mater. **58**, 5789 (2010).
[19]D. Jang and J. R. Greer, Nature Mater. **9**, 215 (2010).
[20]H. B. Ke, P. Wen, H. L. Peng, W. H. Wang, and A. L. Greer, Scr. Mater. **64**, 966 (2011).
[21]T. H. Courtney, *Mechanical Behavior of Materials* (McGraw-Hill Education/China Machine, Beijing, 2004).
[22]W. Flügge, *Viscoelasticity*, 2nd ed. (Springer-Verlag, Berlin, 1975).
[23]C. A. Angell, Science **267**, 1924 (1995).
[24]R. Busch, E. Bakke, and W. L. Johnson, Acta Mater. **46**, 4725 (1998).
[25]I. Gallino, J. Schroers, and R. Busch, J. Appl. Phys. **108**, 063501 (2010).
[26]H. B. Ke, W. H. Wang, and Y. Wu (to be published).
[27]H. B. Yu, W. H. Wang, H. Y. Bai, Y. Wu, and M. W. Chen, Phys. Rev. B **81**, 220201 (2010).
[28]J. J. Lewandowski and A. L. Greer, Nature Mater. **5**, 15 (2006).
[29]B. Yang, C. T. Liu, and T. G. Nieh, Appl. Phys. Lett. **88**, 221911 (2006).
[30]Y. H. Liu, C. T. Liu, W. H. Wang, A. Inoue, T. Sakurai, and M. W. Chen, Phys. Rev. Lett. **103**, 065504 (2009).
[31]L. S. Huo, H. Y. Bai, X. K. Xi, D. W. Ding, D. Q. Zhao, W. H. Wang, R. J. Huang, and L. F. Li, J. Non-Cryst. Solids **357**, 3088 (2011).
[32]Y. H. Liu, G. Wang, R. J. Wang, D. Q. Zhao, M. X. Pan, and W. H. Wang, Science **315**, 1385 (2007).
[33]W. H. Wang, J. Appl. Phys. **110**, 053521 (2011).